Physica B 456 (2015) 57–65

Contents lists available at ScienceDirect

Physica B

journal homepage: www.elsevier.com/locate/physb

Frequency dependent figure-of-merit in cylindrical thermoelectric nanodevices

A. Sellitto

Department of Mathematics, Computer Science and Economics, University of Basilicata, Campus Macchia Romana, 85100 Potenza, Italy

ARTICLE INFO

Article history:
Received 21 July 2014
Received in revised form
11 August 2014
Accepted 15 August 2014
Available online 23 August 2014

Keywords:
Figure-of-merit
Thermoelectric effects
Thermoelectric nanodevice
Frequency-dependent situations

ABSTRACT

We use a theoretical mesoscopic model accounting for memory and nonlocal effects in thermoelectricity in order to investigate how the figure-of-merit in cylindrical thermoelectric nanodevices is conditioned in frequency-dependent situations. Two different situations, regarding the relative values of the particles' mean-free path and the characteristic size of the system, are analyzed. It is shown that in both situations the performances of the thermoelectric devices are reduced. However, nonlocal effects may be used as an aiding tool to have less marked reductions in those performances.

© 2014 Elsevier B.V. All rights reserved.

1. Introduction

Alternative power sources based on energy harvesting are promising candidates to substitute batteries due to their ability to extract unlimited power from the environment or secondary processes, as well as to attain fully autonomous systems without periodical human interventions. Due to the large amount of residual heat yielding from the current energy generation technology based on fossil fuels, thermoelectric energy harvesters have received special attention in recent years. Thermoelectric devices offer a very attractive source of energy since they do not have moving parts, create pollution, or make noise.

In practical applications, the definition of a "good thermoelectric device" is usually related to the dimensionless product ZT, with T being the operating temperature, and Z the so-called figure-of-merit, defined as

$$Z = \frac{\epsilon^2 \sigma_e}{\lambda} \tag{1}$$

wherein ϵ is the Seebeck coefficient, σ_e the electrical conductivity, and λ the total thermal conductivity.

In thermoelectric materials heat is carried both by phonons and by electrons, and by definition, in Eq. (1) the total thermal conductivity is such that

$$\lambda = \lambda_p + \lambda_e \tag{2}$$

with λ_p being the phonon contribution to the thermal conductivity, whereas λ_e means the electron contribution to it [1–3].

Since the higher ZT, the higher the efficiency of a thermoelectric device, in order to widen the applications of thermoelectric power generators, in the last decades there has been a tremendous amount of researches to improve the values of ZT beyond those of bulk materials, which show, instead, low efficiencies. However, ZT has remained approximately equal to 1 for the past several decades in the case of archetype materials at all temperature ranges. These materials include antimony (Sb_2Te_3) and bismuth tellurides (Be_2Te_3) for room temperature applications, lead telluride (PbTe) at moderate temperatures, and silicon-germanium (SiGe) alloys at high temperatures.

One of the primary challenges in developing advanced thermoelectric materials is decoupling ϵ, σ_e and λ which are typically strongly interdependent in such a way that an increase in ϵ usually results in a decrease in σ_e, and a decrease in σ_e produces a decrease in the electronic contribution to λ, following from the Wiedemann–Franz law.

Indeed, if the characteristic dimension of the material (or the system) is shortened, the new variable of length scale also becomes available for the control of the materials' properties. In particular, as the system size decreases and approaches nanometer length scales, new opportunities are allowed to vary the aforementioned parameters quasi-independently. Nanomaterials, therefore, provide an interesting avenue to achieve this goal, for example, making nanocomposites, adding nanoparticles to a bulk material, or employing one-dimensional nanostructures [4,5]. Nanosystems offer the possibility of an additional control of the transport coefficients [6–9]. For instance, whenever the characteristic size of the system is comparable to the mean-free path (mfp) ℓ of the different heat carriers (phonons, electrons, holes, etc.) it is known that a thermal conductivity reduction can be realized over

E-mail address: antsel@gmail.com

http://dx.doi.org/10.1016/j.physb.2014.08.012
0921-4526/© 2014 Elsevier B.V. All rights reserved.

a wide temperature range, or the power factor can be increased at the same time by increasing ϵ more than σ_e is decreased [10,11].

Although from experimental evidences it is very clear the importance of using nanotechnologies in thermoelectricity, the search of a very good thermoelectric device is still far from its final solution. This principally because the physics at nanoscale still presents several dark points, as for instance the role played by memory, nonlocal and nonlinear effects [12,13,6,8,7].

In particular memory effects may drastically influence, for example, the behavior of nanodevices at high frequencies [14,15]. In fact, in the simplest description of relaxational effects in the bulk for phonon heat transport, the heat flux $\mathbf{q}$ is given by the Maxwell–Cattaneo equation

$$\tau_p D_t \mathbf{q} + \mathbf{q} = -\lambda \nabla T \tag{3}$$

where τ is the relaxation time due to the resistive interactions (momentum not conserved) between the heat carriers, and the symbol D_t means the material derivative. The Fourier transform of this equation leads to an effective frequency-dependent thermal conductivity of the form

$$\lambda^{\text{eff}}(\omega) = \frac{\lambda}{1+(\omega\tau_p)^2} \tag{4}$$

which points out that the higher the frequency ω, the smaller the thermal conductivity.

This result may be interesting for thermoelectric applications, since small values of the thermal conductivity could lead to an enhancement of Z, according to Eq. (1).

Indeed, the analysis and modelization of heat transport in nanosystems are more complex since it is also required to pay a special attention to the boundary conditions [3]. The interest on wall effects, related to phonon–wall interactions [16,17], recently surged with the synthesis of nanowires with rough walls [18,19]. Furthermore, in thermoelectricity, one has to monitor also the frequency behavior of other material functions. Therefore, in the present paper, from a phenomenological point of view, we explore the frequency dependence of Z in cylindrical nanowires in order to point out whether the performances of thermoelectric devices may be enhanced by coupling relaxational and nonlocal effects in high-frequencies situations, or not. It is important to note that the approach used in the present paper rests on a mesoscopic level, as our main aim is to provide a first rough (but simple to obtain) estimation of the response of a thermoelectric device in frequency-dependent situations. In this sense, the present analysis should be only viewed as a first step towards more detailed microscopic scrutinies.

The structure of the paper is the following. In Section 2 we introduce transport equations with relaxational and nonlocal effects in heat and electric transport. In Section 3 we derive the frequency-dependent behavior of the figure-of-merit by modeling the interactions of the different heat carriers with the boundaries. In Section 4 we draw the main conclusions.

2. Enhanced thermoelectric equations with relaxational and nonlocal effects

On microscopic grounds both electrons and phonons may be viewed as a free-particle gas in a box [20]. In nonequilibrium mechanics, the statistical behavior of a thermodynamic system far from its thermodynamic equilibrium is described through the Boltzmann transport equation (BTE), which in the relaxation-time approximation reads:

$$\partial_t f + \cdot \nabla_{\mathbf{r}} f + \frac{\mathbf{F}}{m} \cdot \nabla_{\mathbf{v}} f = -\frac{f - f_0}{\tau} \tag{5}$$

wherein the subscripts $\mathbf{r}$ and $\mathbf{v}$ in the nabla operators represent the variables of the gradient, i.e., they are the position and the velocity of a set of particles, respectively. Moreover, in Eq. (5) $f(\mathbf{r};\mathbf{v};t)$ is the probably-density function, f_0 represents the equilibrium distribution of the carriers, and $\tau(\mathbf{r};\mathbf{k})$ is their relaxation time, $\mathbf{k}$ being the wave vector of the particle. In the BTE, f_0 is given by the Bose–Einstein distribution function (BEdf) in the case of phonons, i.e.,

$$f_0 = (e^{\hbar\nu/k_B T} - 1)^{-1}$$

wherein $\hbar = h/(2\pi)$ with h being the Planck constant, ν is the angular frequency, and k_B is the Boltzmann constant. In the case of electrons, instead, f_0 is expressed by the Fermi-Dirac distribution function (FDdf), i.e.,

$$f_0 = (e^{(\varepsilon_i - \mu_e)/k_B T} + 1)^{-1}$$

with ε_i being the energy of the single-particle state, and μ_e is the chemical potential.

Indeed, it is possible to find several situations, as for example whenever the quantities $(\varepsilon_i - \mu_e)$ and $\hbar\nu$ are much larger than $k_B T$, in which one can ignore the ± 1 in the denominator of f_0, in order that the BEdf and the FDdf reduce to the Boltzmann distribution function [20]. In these cases, on intuitively ground, the solution of the BTE both for phonons, and for electrons would lead to equations showing the same mathematical behavior.

Starting from these considerations and in accordance with the basic principles of Extended Irreversible Thermodynamics [7,6], in Refs. [21,3] the following generalized transport equations to describe heat and electric transport with thermoelectric coupling have been considered:

$$\tau_p D_t \mathbf{q}^{(p)} + \mathbf{q}^{(p)} = -\lambda_p \nabla T + \ell_p^2 (\nabla^2 \mathbf{q}^{(p)} + 2\nabla\nabla \cdot \mathbf{q}^{(p)}) \tag{6a}$$

$$\tau_e D_t \mathbf{q}^{(e)} + \mathbf{q}^{(e)} = -(\lambda_e + \epsilon \Pi \sigma_e)\nabla T + \ell_e^2 (\nabla^2 \mathbf{q}^{(e)} + 2\nabla\nabla \cdot \mathbf{q}^{(e)}) + \Pi \sigma_e \mathbf{E} \tag{6b}$$

$$\tau_e D_t \mathbf{i} + \mathbf{i} = \sigma_e (\mathbf{E} - \epsilon \nabla T) + \ell_e^2 (\nabla^2 \mathbf{i} + 2\nabla\nabla \cdot \mathbf{i}) \tag{6c}$$

In these equations $\mathbf{i}$ is the electric-current density, $\mathbf{E}$ is the electric field, and Π is the Peltier coefficient. The basic idea lying under these equations is that the local heat flux shows both a phonon contribution $\mathbf{q}^{(p)}$, and an electron contribution $\mathbf{q}^{(e)}$ in such a way that $\mathbf{q} = \mathbf{q}^{(p)} + \mathbf{q}^{(e)}$.

Referring the readers to Section 4 for more comments about Eqs. (6), here let us only comment about the different material functions included therein. In Eqs. (6) τ_p and τ_e represent, respectively, the relaxation time due to phonons interactions and that due to electrons interactions. In more detail, the relaxation time τ_p may be related to the resistive mechanisms between the different particles in such a way that, through the Matthiessen rule, it is given as

$$\tau_p^{-1} = \tau_u^{-1} + \tau_i^{-1} + \tau_d^{-1} + \tau_{p-w}^{-1} + \tau_{e-p}^{-1}$$

where τ_u is the relaxation time of umklapp-phonon collisions, τ_i the relaxation time of phonon-impurity collisions, τ_d the relaxation time of phonon-defect collisions, and τ_{e-p} is the electron–phonon scattering-time [22]. Similarly, the electron relaxation time τ_e may be defined as

$$\tau_e^{-1} = \tau_{e-e}^{-1} + \tau_{e-p}^{-1}$$

with τ_{e-e} being the electron–electron scattering-time [23,24]. In principle, in defining both τ_p and τ_e further relaxation times, accounting for the phonon–wall and electron–wall interactions, should be taken into account. In our approach these interactions will be introduced by means of suitable boundary conditions in Section 3.

Moreover, in Eq. (6a) ℓ_p means the mfp of phonons, which is related both to resistive, and to the normal scattering of phonons

[25] since $\ell_p^2 = v_p^2 \tau_n \tau_p/5$, τ_n being the relaxation time of normal collisions, and v_p being the average phonon speed. In Eqs. (6b) and (6c), instead, ℓ_e is the mfp of electrons in the bulk [26], which is dominated by electron and phonon scattering in such a way that $\ell_e = v_F \tau_e$, with v_F as the Fermi velocity. Indeed, ℓ_e can be also expressed by the Drude formula [27].

In Eqs. (6) the second-order spatial derivatives of the fluxes allow to account for nonlocal effects, whereas their time derivatives introduce memory and relaxational effects. It is easy to recognize that in the absence of nonlocal and memory effects, from Eqs. (6) the classical thermoelectric equations

$$\mathbf{q} = -\lambda \nabla T + \Pi \mathbf{i}$$
$$\mathbf{i} = \sigma_e(\mathbf{E} - \epsilon \nabla T)$$

are recovered once Eqs. (6a) and (6b) are summed.

For the sake of a theoretical completeness, since the model Eqs. (6) lie on the idea that the heat carriers form a gas-like mixture flowing through the crystal lattice, we observe that each heat carrier obeys the same balance equations as the single component of the mixture [3], namely, the following further equations hold:

$$D_t u^{(p)} + \nabla \cdot \mathbf{q}^{(p)} = 0 \tag{8a}$$

$$D_t u^{(e)} + \nabla \cdot \mathbf{q}^{(e)} = \mathbf{E} \cdot \mathbf{i} \tag{8b}$$

where $u^{(p)}$ and $u^{(e)}$ are the partial internal energies (of phonons and electrons, respectively), and the term $\mathbf{E} \cdot \mathbf{i}$ accounts for the Joule dissipation. The rate of the electric charge density $\varrho^{(e)}$, instead, obeys the charge conservation law, i.e.,

$$D_t \varrho^{(e)} + \nabla \cdot \mathbf{i} = 0 \tag{9}$$

which, together with Eqs. (8), determines the evolution of $u^{(p)}$, $u^{(e)}$ and $\varrho^{(e)}$, once the evolutions of the corresponding fluxes $\mathbf{q}^{(p)}$, $\mathbf{q}^{(e)}$ and $\mathbf{i}$ are known.

In the next section, we will analyze how the dynamical terms in Eqs. (6) (i.e., $\tau_p D_t \mathbf{q}^{(p)}$, $\tau_e D_t \mathbf{q}^{(e)}$, and $\tau_e D_t \mathbf{i}$), complemented with suitable boundary conditions (accounting for the interactions between the different heat carriers and the walls), may influence the figure-of-merit in frequency-dependent situations.

3. Frequency dependent figure-of-merit in cylindrical nanowires

Owing to the fast progress in the fabrication of nanoscale devices and the predictions of an improvement in the figure-of-merit of low dimensional semiconducting structures, many efforts have been made in the thermoelectric field via engineering at the nanoscale. Although the main research line rests on the search of suitable new materials with high values of Z, also new strategies should be desirable. Motivated by this, in Ref. [3] the authors have studied the size dependency of the figure-of-merit, complementing Eqs. (6) with suitable boundary conditions accounting for the interactions between the different heat carriers and the lateral walls of the system in steady-state situations. That analysis clearly pointed out the role played by nonlocal effects, and their possible use to enhance the performances of a thermoelectric device. However, at nanoscale, also memory and relaxational effects may be important, especially in unsteady-state situations [14]. Therefore, in the present section, we try to estimate how the figure-of-merit in cylindrical nanowires may depend on the frequency of perturbations. In particular, in order to analyze the possible consequences of accounting for relaxational effects in practical applications, here we apply the theoretical model in Eqs. (6) in the concrete situation of a nanowire which is characterized both by a (constant) circular transversal section of radius R, and by a longitudinal length L much larger than the latter. We will perform our analysis in the following two possible cases:

(i) when R is such that $\ell_e < R < \ell_p$;
(ii) when R is such a way that $R < \ell_e, \ell_p$.

In both cases we assume that the temperature difference (applied through the ends of the system) and the electric field may vary in the following sinusoidal way:

$$\Delta T(\omega; t) = \Delta T_0 e^{j\omega t} \tag{10a}$$

$$E(\omega; t) = E_0 e^{j\omega t} \tag{10b}$$

ω being the angular frequency of the perturbations, while ΔT_0 and E_0 are stationary reference levels. Eqs. (10) imply that both the temperature, and the electric field are homogeneous across every transversal section of the nanowire, but with an amplitude changing in time. Moreover, the former depends on the longitudinal position, whereas the latter is independent of it.

3.1. Case of study: $\ell_e < R < \ell_p$

In Si or Bi_2Te_3 the phonon mfp is generally one order of magnitude larger than the electron one [28,19]. Therefore, when these materials are used in building up thermoelectric devices, a realistic assumption is to assume that the radius of the transversal section is larger than ℓ_e, but smaller than ℓ_p.

In this case the phonons undergo the hydrodynamic regime, and the electrons the usual resistive regime. In hydrodynamic regime the transport is ballistic [14], and in the evolution equation of the corresponding heat flux, i.e., in Eqs. (6a), the second-order spatial derivatives play the main role, in such a way that their contribution is predominant with respect to that of the heat flux itself [17,3]. Moreover, in such a situation, the heat-flux profile in a given transversal section is strongly dependent on the characteristic size of the system [29,17]. In the resistive regime, instead, the transport is diffusive [14], and the second-order spatial derivatives of the diffusive flux can be neglected, since the main role in the evolution equation is played by the diffusive flux itself. In this case, the dependence of the single diffusive flux on the characteristic size is realistically negligible.

From the practical point of view, previous considerations allow to conclude that whenever $\ell_e < R < \ell_p$ Eqs. (6) may be reduced as

$$\tau_p D_t \mathbf{q}^{(p)} = -\lambda_p \nabla T + \ell_p^2 (\nabla^2 \mathbf{q}^{(p)} + 2 \nabla \nabla \cdot \mathbf{q}^{(p)}) \tag{11a}$$

$$\tau_e D_t \mathbf{q}^{(e)} + \mathbf{q}^{(e)} = -(\lambda_e + \epsilon \Pi \sigma_e) \nabla T + \Pi \sigma_e \mathbf{E} \tag{11b}$$

$$\tau_e D_t \mathbf{i} + \mathbf{i} = \sigma_e (\mathbf{E} - \epsilon \nabla T) \tag{11c}$$

In order to keep the calculations down to a reasonable level, in using Eqs. (11) we assume that both the heat flux, and the electrical current may only flow longitudinally through the system. Moreover, in the present case, we assume that the bulk profiles for the different diffusive fluxes are given by

$$q_{\mathrm{b}}^{(p)}(r; \omega; t) = q_{\mathrm{b},0}^{(p)} \left(\frac{R^2 - r^2}{4 \ell_p^2} \right) e^{j\omega t} \tag{12a}$$

$$q_{\mathrm{b}}^{(e)}(\omega; t) = q_{\mathrm{b},0}^{(e)} e^{j\omega t} \tag{12b}$$

$$i_{\mathrm{b}}(\omega; t) = i_{\mathrm{b},0} e^{j\omega t} \tag{12c}$$

that is, we assume that they have amplitudes which periodically deviate in time from the stationary reference levels $q_{\mathrm{b},0}^{(p)}$, $q_{\mathrm{b},0}^{(e)}$ and $i_{\mathrm{b},0}$, but they are independent of the longitudinal position. It is worth noticing that Eq. (12a) prescribes that, in a given section and

time, $q_{\rm b}^{(p)}$ essentially keeps the parabolic behavior corresponding to the Poiseuille phonon flow [29,17], whereas $q_{\rm b}^{(e)}$ and $i_{\rm b}$ are homogeneous. These assumptions follow from the considerations above about the different transport regimes.

We also note that $q_{\rm b,0}^{(p)}$, $q_{\rm b,0}^{(e)}$ and $i_{\rm b,0}$ in Eqs. (12) are related to ΔT_0 and E_0 in Eqs. (10). In fact, combining Eqs. (10) and (12), by straightforward calculations, we have

$$q_{\rm b,0}^{(p)} = \left[\frac{\lambda_p + 2j\omega c_v^{(p)}\ell_p^2}{1+j\omega\tau_p\left(\frac{R^2-r^2}{4\ell_p^2}\right)}\right]\frac{\Delta T_0}{L} \tag{13a}$$

$$q_{\rm b,0}^{(e)} = q_{\rm b,0}^{(e,\Delta T)} + q_{\rm b,0}^{(e,E)} = \left(\frac{\lambda_e + e\Pi\sigma_e}{1+j\omega\tau_e}\right)\frac{\Delta T_0}{L} + \left(\frac{\Pi\sigma_e}{1+j\omega\tau_e}\right)E_0 \tag{13b}$$

$$i_{\rm b,0} = i_{\rm b,0}^{(\Delta T)} + i_{\rm b,0}^{(E)} = \left(\frac{e\sigma_e}{1+j\omega\tau_e}\right)\frac{\Delta T_0}{L} + \left(\frac{\sigma_e}{1+j\omega\tau_e}\right)E_0 \tag{13c}$$

wherein $c_v^{(p)}$ is the specific heat at constant volume of phonons, which may be related to the temperature through the usual constitutive assumption $u^{(p)} = c_v^{(p)}T$. It seems worth observing that in the whole generality, $u^{(p)}$ should also be also q and i dependent. However, although more refined assumptions may be introduced, here we use that assumption in order to deal only with the simplest situation, emphasizing the physical idea. In particular, that constitutive relation, combined with Eq. (8a), has been used to express $\nabla\nabla\cdot\mathbf{q}^{(p)}$ in terms of the temperature gradient in deriving Eq. (13a).

Since the electrons may be dragged both by a temperature gradient, and by an electric field, in Eq. (13b) the two different contributions to the bulk electron heat flux $q_{\rm b,0}^{(e)}$ have been explicitly expressed: that only due to the temperature gradient (i.e., $q_{\rm b,0}^{(e,\Delta T)}$) and that only due to the electric field (i.e., $q_{\rm b,0}^{(e,E)}$). Analogously, in Eq. (13c) appear the two different contributions to the bulk electric-current density $i_{\rm b,0}$, namely, $i_{\rm b,0}^{(\Delta T)}$ which is due to the temperature gradient, and $i_{\rm b,0}^{(E)}$ which is due to the presence of the electric field.

As we are analyzing a situation in which the phonons undergo the hydrodynamic regime, we have to pay a special attention on the interactions between them and the lateral walls [29,30]. This can be done, for example, by assuming that the full-local phonon contribution to the heat flux is given as

$$q^{(p)} = q_{\rm b}^{(p)} + q_{\rm w}^{(p)} \tag{14}$$

where $q_{\rm w}^{(p)}$ is the wall contribution which is progressively tuned down far from the walls. Note that in general, in accounting for boundary effects, it should be admitted that $q^{(p)}$ takes the value $q_{\rm b}^{(p)}$ in the bulk, and the value $q_{\rm w}^{(p)}$ at the walls. However, since boundary conditions strongly determine the behavior of a system, one could nevertheless expect that the thermal conductivity is only dependent on $q_{\rm b}^{(p)}$ in the bulk, and on the value of $q_{\rm w}^{(p)}$ at the boundary of the wall. Indeed, from the physical point of view, the boundary is never a true surface, but rather a thin layer (the so-called Knudsen layer), whose dimension is of the order of magnitude of the mfp of the heat carriers. On the other hand, since $R < \ell_p$, the Knudsen layer pervades the whole system, so that the heat flux on the boundary (i.e., in the phonon Knudsen layer) is superposed to the heat flux in the bulk. This fact suggests to assume Eq. (14) to estimate the overall heat flux, and suppose that the thermal conductivity depends on it. Moreover, whenever $R < \ell_p$, we are also allowed to assume that $q_{\rm w}^{(p)}$ attains the same value in each point of the transversal section.

No wall contributions are introduced, instead, for the full-local values of $q^{(e)}$ and i which, therefore, coincide with their corresponding bulk values. Along with previous observations about the phonon Knudsen layer, in fact, the electron–wall interactions should be felt in a further thin layer near the walls, the characteristic size of which in of the order of ℓ_e. This zone, which for homogeneity of nomenclature we call electron Knudsen layer, is less wide with respect to the phonon Knudsen layer, since we are assuming that $\ell_e < R$. Therefore, in this case, we do not commit a significant error in admitting that the wall contributions to $q^{(e)}$ and i are vanishingly small.

These considerations allow also to understand that the particle-wall interactions are strictly related to nonlocal effects, since they do not have any relevance whenever nonlocal effects may be neglected.

In view of the dynamical form of $q_{\rm b}^{(p)}$, in the same way as above we assume that the wall contribution is given by

$$q_{\rm w}^{(p)}(\omega;t) = q_{\rm w,0}^{(p)} e^{j\omega t} \tag{15}$$

wherein, in a first-order approximation in space, the reference amplitude value $q_{\rm w,0}^{(p)}$ can be obtained by the following constitutive equation [29,17,30]:

$$\tau_{\rm w}^{(p)} D_t q_{\rm w}^{(p)} + q_{\rm w}^{(p)} = C_p \ell_p \left(\frac{\partial q_{\rm b}^{(p)}}{\partial r}\right)_{r=R} \tag{16}$$

In Eq. (16) $\tau_{\rm w}^{(p)}$ means the relaxation time accounting for the phonon–wall collisions. In principle, it may be estimated, for example, by the usual Matthiessen rule as

$$\tau_{\rm w}^{-1} = \tau_{\rm spec}^{-1} + \tau_{\rm diff}^{-1}$$

where $\tau_{\rm spec}$ and $\tau_{\rm diff}$ are, respectively, the characteristic times of specular and diffusive reflections [29]. Indeed, as a function of the characteristic features of a wall (i.e., the square value of the roughness fluctuations and the average distance between roughness peaks [31]), in Ref. [32] the authors provided a possible way of estimating that relaxation time in terms of the total frequency of collisions between phonons and walls.

Moreover, in Eq. (16) C_p means a dimensionless coefficient accounting for the rate of reflections (specular and diffusive) of phonons [29,3]. In Ref. [29] the authors provided a simple model to estimate it as a function of the temperature and of the wall features. In Ref. [33], instead, the following more refined model for C_p may be found:

$$C_p = \frac{2}{3}\left[\frac{(3-\xi f^3)}{\xi} - \frac{3}{2}\frac{(1-f^2)}{{\rm Kn}_p}\right]$$

with $f = \min[1/{\rm Kn}_p, 1]$, ${\rm Kn}_p = \ell_p/R$ being the phonon Knudsen number, and ξ a suitable accommodation parameter. This coefficient represents the portion of the total wall-colliding particles that are diffusively reflected back by wall and have a bulk velocity equal to the wall velocity after collisions. In principle, C_p values should be taken in the range [0;1]. In fact, since C_p also turns out the relative importance of $q_{\rm w}^{(p)}$ with respect to $q_{\rm b}^{(p)}$ in Eq. (14), in general the C_p values should be small in such a way that $q_{\rm b}^{(p)}$ always remains the main contribution to the full-local phonon heat flux in Eq. (14).

Note that Eq. (16) has to be meant as a relaxational generalization of the boundary condition used in Ref. [3] (see Eqs. (11) therein) in the spirit of the Maxwell–Cattaneo equation (3), wherein a relaxational term (including the time derivative of the heat flux) is added to the usual Fourier heat-transport equation. Though in the usual applications the term $\tau_{\rm w}^{(p)} D_t q_{\rm w}^{(p)}$ is vanishingly small, for high frequencies it may be obviously important, and therefore its incorporation in Eq. (16) seems logical. Referring the readers to Section 4 for further comments about Eq. (16), we observe that a simple and systematic derivation of that equation can be found in Ref. [30] by using the tools of Extended Irreversible Thermodynamics [7].

The coupling of Eqs. (13a) and (15) with Eq. (16) turns out that the amplitude of the wall contribution to the phonon heat flux is

$$q_{\mathrm{w},0}^{(p)}=\frac{C_p}{2\mathrm{Kn}_p}\left(\frac{\lambda_p+2j\omega c_v^{(p)}\ell_p^2}{1+j\omega\tau_{\mathrm{w}}^{(p)}}\right)\frac{\Delta T_0}{L} \tag{17}$$

If we define the following effective quantities

$$\lambda_p^{\mathrm{eff}}=Re\left\{\frac{L}{\Delta T}\left(\frac{Q_{\mathrm{tot}}^{(p)}}{\pi R^2}\right)\right\}=Re\left\{\frac{L}{\Delta T}\left[\frac{\int_0^R 2\pi r(q_{\mathrm{b}}^{(p)}+q_{\mathrm{w}}^{(p)})\,dr}{\pi R^2}\right]\right\} \tag{18a}$$

$$(\lambda_e+\epsilon\Pi\sigma_e)^{\mathrm{eff}}=Re\left\{\frac{L}{\Delta T}\left(\frac{Q_{\mathrm{tot}}^{(e,\Delta T)}}{\pi R^2}\right)\right\}=Re\left\{\frac{L}{\Delta T}\left[\frac{\int_0^R 2\pi r q_{\mathrm{b}}^{(e,\Delta T)}dr}{\pi R^2}\right]\right\} \tag{18b}$$

$$(\Pi\sigma_e)^{\mathrm{eff}}=Re\left\{\frac{1}{E}\left(\frac{Q_{\mathrm{tot}}^{(e,E)}}{\pi R^2}\right)\right\}=Re\left\{\frac{1}{E}\left[\frac{\int_0^R 2\pi r q_{\mathrm{b}}^{(e,E)}dr}{\pi R^2}\right]\right\} \tag{18c}$$

$$(\epsilon\sigma_e)^{\mathrm{eff}}=Re\left\{\frac{L}{\Delta T}\left(\frac{J_{\mathrm{tot}}^{(\Delta T)}}{\pi R^2}\right)\right\}=Re\left\{\frac{L}{\Delta T}\left[\frac{\int_0^R 2\pi r i_{\mathrm{b}}^{(\Delta T)}dr}{\pi R^2}\right]\right\} \tag{18d}$$

$$\sigma_e^{\mathrm{eff}}=Re\left\{\frac{1}{E}\left(\frac{J_{\mathrm{tot}}^{(E)}}{\pi R^2}\right)\right\}=Re\left\{\frac{1}{E}\left[\frac{\int_0^R 2\pi r i_{\mathrm{b}}^{(E)}dr}{\pi R^2}\right]\right\} \tag{18e}$$

then all the considerations above allow to obtain the following effective coefficients:

$$\lambda_p^{\mathrm{eff}}=2\lambda_p\left(\frac{\mathrm{Kn}_p}{\omega\tau_p}\right)^2\left\{\ln\left[1+\left(\frac{\omega\tau_p}{4\mathrm{Kn}_p^2}\right)^2\right]-12\omega\tau_p\arctan\left(\frac{\omega\tau_p}{4\mathrm{Kn}_p^2}\right)\right\}+6\lambda_p\left\{1+\frac{C_p}{12\mathrm{Kn}_p}\left[\frac{1+6(\omega\tau_p)^2\alpha_p}{1+(\alpha_p\omega\tau_p)^2}\right]\right\} \tag{19a}$$

$$\lambda_e^{\mathrm{eff}}=\frac{\lambda_e}{1+(\omega\tau_e)^2} \tag{19b}$$

$$\sigma_e^{\mathrm{eff}}=\frac{\sigma_e}{1+(\omega\tau_e)^2} \tag{19c}$$

$$\epsilon^{\mathrm{eff}}=\epsilon \tag{19d}$$

$$\Pi^{\mathrm{eff}}=\Pi \tag{19e}$$

wherein $\alpha_p=\tau_{\mathrm{w}}^{(p)}/\tau_p$. For the sake of formal simplicity, in Eq. (19a) we expressed the phonon relaxation time as $\tau_p=\ell_p/v_p$, and we used the usual Ziman limit for the phonon bulk thermal conductivity, i.e., $\lambda_p=c_v^{(p)}\tau_p v_p^2/3$.

It seems interesting to note that the theoretical model described by Eqs. (11) prescribes that only the thermal and the electrical conductivities show effective values that differ from their corresponding bulk values. Moreover, as expected whenever $\ell_e<R<\ell_p$, among them only the phonon contribution to the effective thermal conductivity shows the influence of the radius.

It is easy to see that in the low-frequency limit (that is, whenever $\omega\tau_p\to 0$ and $\omega\tau_e\to 0$) Eqs. (19a)–(19c) reduce to the effective values obtained in Ref. [3] whenever the radius of the transversal section is in the range $[\ell_e;\ell_p]$, that is,

$$\lambda_p^{\mathrm{eff}}=\frac{\lambda_p}{8\mathrm{Kn}_p^2}(1+4C_p\mathrm{Kn}_p)$$
$$\lambda_e^{\mathrm{eff}}=\lambda_e$$
$$\sigma_e^{\mathrm{eff}}=\sigma_e$$

In Fig. 1 we plot the frequency-dependent behaviors of λ_e^{eff}, λ_p^{eff} and σ_e^{eff} (referred to their corresponding bulk values) arising from Eqs. (19a)–(19c) in the case of a p-doped sample of Bi_2Te_3 at 300 K. Furthermore, the combination of Eqs. (1) and (19a)–(19c), is used to plot in the same figure also the behavior of the effective frequency-dependent

$$Z^{\mathrm{eff}}=\frac{(\epsilon^{\mathrm{eff}})^2\sigma_e^{\mathrm{eff}}}{\lambda_p^{\mathrm{eff}}+\lambda_e^{\mathrm{eff}}}$$

referred to its corresponding bulk value.

The values of the different material functions, related to phonons and electrons, we used in the computation are summarized in Table 1. For the sake of computation, we assumed $R=2$ nm. From those values we estimated the following relaxation times:

$$\tau_p=\frac{\ell_p}{v_p}=3.5\times 10^{-13}\ \mathrm{s}$$
$$\tau_e=\frac{\ell_e}{v_F}=2.8\times 10^{-13}\ \mathrm{s}$$
$$\tau_{\mathrm{w}}^{(p)}=\frac{R}{v_p}=2.4\times 10^{-13}\ \mathrm{s}$$

This means that whenever $\omega\tau_p\to 1$, then ω is of the order of THz. Therefore, in Fig. 1 ω spans the usual range of admissible frequencies. Since we are not aware of experimental data to estimate the parameter accounting for the phonon–wall reflections, we used two different admissible values for it, that is, $C_p=0.1$ and $C_p=0.5$.

As it can be seen from Fig. 1, the higher ω, the smaller λ_e^{eff} and σ_e^{eff}. These results are a natural consequence of the electron transport-regime type (i.e., the resistive regime). In the case of the phonon transport regime, instead, the relevance of nonlocal effects leads to an enhancement of λ_p^{eff} for increasing ω. The combination of these behaviors leads to an effective figure-of-merit which is substantially decreasing for increasing frequency, whatever the value of C_p is. However, the smaller C_p, the less marked the decreasing in Z. Therefore, the theoretical model in Eqs. (6) suggests that the performances of a thermoelectric device tend to go worse in frequency-dependent situations.

3.2. Case of study: $R<\ell_e,\ell_p$

Due to the incessant developments in nanotechnology, it should be also possible to face with situations in which the characteristic size of the device is smaller both than the phonon mfp, and than the electron one. In these situations all the heat carriers undergo the hydrodynamic regime, and Eqs. (6) become

$$\tau_p D_t\mathbf{q}^{(p)}=-\lambda_p\nabla T+\ell_p^2(\nabla^2\mathbf{q}^{(p)}+2\nabla\nabla\cdot\mathbf{q}^{(p)}) \tag{20a}$$

$$\tau_e D_t\mathbf{q}^{(e)}=-(\lambda_e+\epsilon\Pi\sigma_e)\nabla T+\ell_e^2(\nabla^2\mathbf{q}^{(e)}+2\nabla\nabla\cdot\mathbf{q}^{(e)})+\Pi\sigma_e\mathbf{E} \tag{20b}$$

$$\tau_e D_t\mathbf{i}=\sigma_e(\mathbf{E}-\epsilon\nabla T)+\ell_e^2(\nabla^2\mathbf{i}+2\nabla\nabla\cdot\mathbf{i}) \tag{20c}$$

In this case, in order to study the frequency-dependent effective figure-of-merit we can still assume that $q_{\mathrm{b}}^{(p)}$ is given by Eq. (12a), which substantially leads to the frequency-dependent effective phonon thermal conductivity (19a), once the phonon–wall interactions are introduced by a wall contribution as in Eq. (16).

Different treatments, instead, are needed for $q_{\mathrm{b}}^{(e)}$ and i_{b}. In fact, since in this case also the electron transport is ballistic, we can no longer assume that those fluxes show profiles which are homogeneous in each transversal section for a fixed time. Therefore, along with previous considerations about Eq. (12a), here we assume that $q_{\mathrm{b}}^{(e)}$ and i_{b} have the following profiles, respectively:

$$q_{\mathrm{b}}^{(e)}(r;\omega;t)=q_{\mathrm{b},0}^{(e)}\left(\frac{R^2-r^2}{4\ell_e^2}\right)e^{j\omega t} \tag{21a}$$

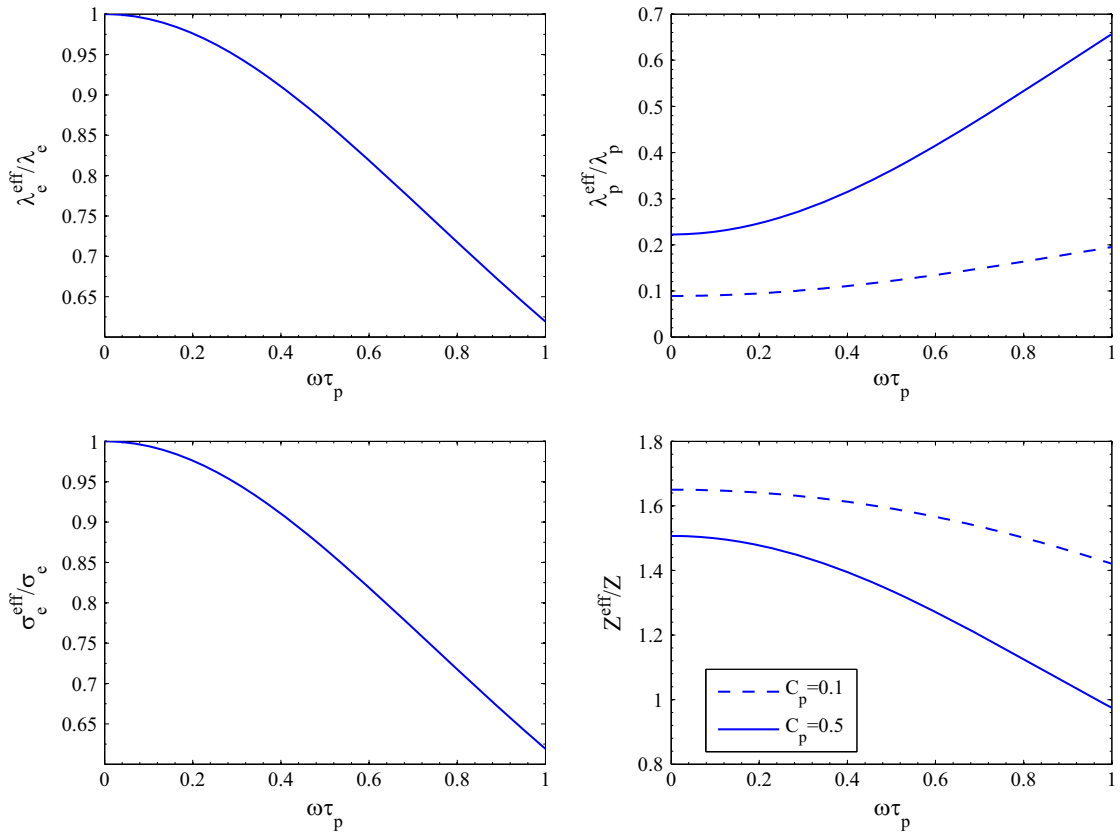

Fig. 1. Frequency-dependent behaviors of $\lambda_e^{\rm eff}$, $\lambda_p^{\rm eff}$, $\sigma_e^{\rm eff}$ and of $Z^{\rm eff}$ in the case of a *p*-doped sample of Bi_2Te_3 at $T=300$ K: theoretical results arising from the theoretical-model equations (11).

Table 1
Values of the material functions for a *p*-doped sample of Bi_2Te_3 at 300 K [28,19].

λ_e (W m^{-1} K^{-1})	λ_p (W m^{-1} K^{-1})	v_F (m s^{-1})	v_p (m s^{-1})	ℓ_e (m)	ℓ_p (m)
2.4	1.6	3.26×10^3	8.43×10^3	9.1×10^{-10}	3.0×10^{-9}

$$i_{\rm b}(\omega;r;t)=i_{\rm b,0}\left(\frac{R^2-r^2}{4\ell_e^2}\right)e^{j\omega t} \tag{21b}$$

namely, we are assuming that $q_{\rm b}^{(e)}$ and $i_{\rm b}$ also keep the parabolic behavior corresponding to the Poiseuille flow [29,17].

In Eqs. (21) the reference-level amplitudes $q_{\rm b,0}^{(e)}$ and $i_{\rm b,0}$ are still strictly related to the temperature difference and the electric field through the end of the system, but in different forms with respect to those predicted by Eqs. (13b), and (13c). In fact, if we combine Eqs. (20b) and (20c) with Eqs. (21), by direct calculations we have that

$$q_{\rm b,0}^{(e)}=q_{\rm b,0}^{(e,\Delta T)}+q_{\rm b,0}^{(e,E)}=\left[\frac{(\lambda_e+\epsilon\Pi\sigma_e)+2j\omega c_v^{(e)}\ell_e^2}{1+j\omega\tau_e\left(\frac{R^2-r^2}{4\ell_e^2}\right)}\right]\frac{\Delta T_0}{L}+\left[\frac{\Pi\sigma_e}{1+j\omega\tau_e\left(\frac{R^2-r^2}{4\ell_e^2}\right)}\right]E_0 \tag{22a}$$

$$i_{\rm b,0}=i_{\rm b,0}^{(\Delta T)}+i_{\rm b,0}^{(E)}=\left[\frac{\sigma_e\epsilon}{1+j\omega\tau_e\left(\frac{R^2-r^2}{4\ell_e^2}\right)}\right]\frac{\Delta T_0}{L}+\left[\frac{\sigma_e}{1+j\omega\tau_e\left(\frac{R^2-r^2}{4\ell_e^2}\right)}\right]E_0 \tag{22b}$$

wherein $c_v^{(e)}$ is the specific heat at constant volume of electrons, which we relate to the average temperature T through the constitutive assumption $u^{(e)}=c_v^{(e)}T$ for a formal simplicity. For the sake of clarity in reading the present paper, we observe that in obtaining Eqs. (22) we combined that constitutive assumption with Eqs. (8b) and (9) in order to write

$$\nabla\nabla\cdot\mathbf{q}^{(e)}=\nabla(-c_v^{(e)}D_tT+\mathbf{E}\cdot\mathbf{i})\approx c_v^{(e)}D_t\Delta T/L$$

once the further simplifying assumption of vanishing value of $D_t\varrho^{(e)}$ in Eq. (9) is made.

Since now we are assuming that R is also smaller than ℓ_e, here we can no longer neglect the influence of the electron–wall interactions [3]. In other words, in the present case we have that also the electron Knudsen layer pervades the whole transversal section. Therefore, in analogy with Eqs. (14), here we assume that the full-local values of $q_{\rm b}^{(e)}$ and $i_{\rm b}$ are given by

$$q^{(e)}=q_{\rm b}^{(e)}+q_{\rm w}^{(e)} \tag{23a}$$

$$i=i_{\rm b}+i_{\rm w} \tag{23b}$$

To cope with high-frequencies situations, still in analogy with what supposed for the phonon–wall heat flux, we assume that the wall contributions $q_{\rm w}^{(e)}$ and $i_{\rm w}$ in Eqs. (23) show the following dynamical behaviors:

$$q_{\rm w}^{(e)}(\omega;t)=q_{\rm w,0}^{(e)}e^{j\omega t} \tag{24a}$$

$$i_{\rm w}(\omega;t)=i_{\rm w,0}e^{j\omega t} \tag{24b}$$

with the reference amplitudes $q^{(e)}_{w,0}$ and $i_{w,0}$ satisfying the dynamical constitutive assumptions

$$\tau^{(e)}_w D_t q^{(e)}_w + q^{(e)}_w = C_e \ell_e \left(\frac{\partial q^{(e)}_b}{\partial r}\right)_{r=R} \tag{25a}$$

$$\tau^{(e)}_w D_t i_w + i_w = C_e \ell_e \left(\frac{\partial i_b}{\partial r}\right)_{r=R} \tag{25b}$$

wherein $\tau^{(e)}_w$ is a relaxation-time due to electron–wall interactions, and C_e turns out the rate of reflected electrons. They substantially play analogous roles of $\tau^{(p)}_w$ and C_p, respectively. In particular, once Eqs. (24) are introduced into Eqs. (25), by straightforward calculations one has

$$q^{(e)}_{w,0} = q^{(e,\Delta T)}_{w,0} + q^{(e,E)}_{w,0} = \frac{C_e}{2o\mathrm{Kn}_e}\left[\left(\frac{\lambda_e + \epsilon\Pi\sigma_e + 2j\omega c^{(e)}_v \ell^2_e}{1+j\omega\tau^{(e)}_w}\right)\frac{\Delta T_0}{L} + \left(\frac{\Pi\sigma_e}{1+j\omega\tau^{(e)}_w}\right)E_0\right] \tag{26a}$$

$$i_{w,0} = i^{(\Delta T)}_{w,0} + i^{(E)}_{w,0} = \frac{C_e}{2\mathrm{Kn}_e}\left[\left(\frac{\epsilon\sigma_e}{1+j\omega\tau^{(e)}_w}\right)\frac{\Delta T_0}{L} + \left(\frac{\sigma_e}{1+j\omega\tau^{(e)}_w}\right)E_0\right] \tag{26b}$$

where $\mathrm{Kn}_e = \ell_e/R$ is the electron Knudsen number.

Then, by means of Eqs. (18b)–(18e), whenever $R < \ell_e$ we obtain that the frequency-dependent effective values of the electron thermal conductivity and of the electrical conductivity in Eqs. (19b) and (19c) become

$$\lambda^{\mathrm{eff}}_e = 2\lambda_e\left(\frac{\mathrm{Kn}_e}{\omega\tau_e}\right)^2\left\{\ln\left[1+\left(\frac{\omega\tau_e}{4\mathrm{Kn}^2_e}\right)^2\right] - 12\omega\tau_e \arctan\left(\frac{\omega\tau_e}{4\mathrm{Kn}^2_e}\right)\right\} + 6\lambda_e\left\{1+\frac{C_e}{12\mathrm{Kn}_e}\left[\frac{1+6(\omega\tau_e)^2\alpha_e}{1+(\alpha_e\omega\tau_e)^2}\right]\right\} \tag{27a}$$

$$\sigma^{\mathrm{eff}}_e = 2\sigma_e\left\{\left(\frac{\mathrm{Kn}_e}{\omega\tau_e}\right)^2\ln\left[1+\left(\frac{\omega\tau_e}{4\mathrm{Kn}^2_e}\right)^2\right] + \frac{C_e}{4\mathrm{Kn}_e}\left[\frac{1}{1+(\alpha_e\omega\tau_e)^2}\right]\right\} \tag{27b}$$

whereas the effective Seebeck and Peltier coefficients still keep their corresponding bulk values. Note that in deriving Eqs. (27) we expressed the electron relaxation time as $\tau_e = \ell_e/v_F$, and the electron bulk thermal conductivity as $\lambda_e = c^{(e)}_v \tau_e v^2_F/3$. Moreover, in those equations we set $\alpha_e = \tau^{(e)}_w/\tau_e$.

It is easy to see that in the low-frequency limit (that is, whenever $\omega\tau_p \to 0$ and $\omega\tau_e \to 0$) Eqs. (27) reduce to the effective values obtained in Ref. [3] whenever $R < \ell_e, \ell_p$, that is,

$$\lambda^{\mathrm{eff}}_e = \frac{\lambda_e}{8\mathrm{Kn}^2_e}(1+4C_e\mathrm{Kn}_e)$$

$$\sigma^{\mathrm{eff}}_e = \frac{\sigma_e}{8\mathrm{Kn}^2_e}(1+4C_e\mathrm{Kn}_e)$$

In Fig. 2 we plot the frequency-dependent behaviors of λ^{eff}_e, λ^{eff}_p and σ^{eff}_e (referred to their corresponding bulk values) arising from the theoretical model in Eqs. (6) in the case of a p-doped sample of Bi_2Te_3 at 300 K, whenever the radius of the transversal section is smaller both than ℓ_p, and ℓ_e. In that figure the behavior of the effective frequency-dependent Z^{eff}, referred to its corresponding bulk value Z, is also plotted. For the sake of computation, in this case we assumed $R = 0.5$ nm which leads to the following relaxation times of heat carriers-walls interactions:

$$\tau^{(p)}_w = \frac{R}{v_p} = 5.9\times10^{-14}\ \mathrm{s}$$

$$\tau^{(e)}_w = \frac{R}{v_F} = 1.5\times10^{-13}\ \mathrm{s}$$

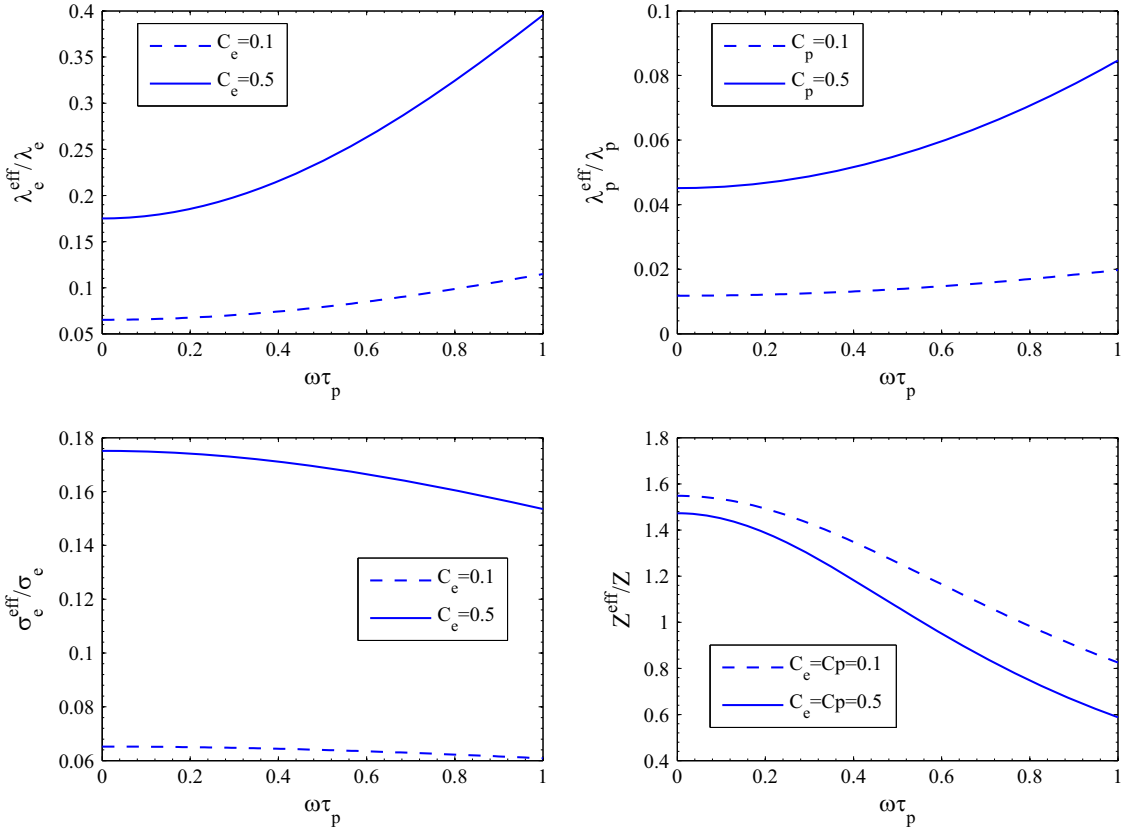

Fig. 2. Frequency-dependent behaviors of λ^{eff}_e, λ^{eff}_p, σ^{eff}_e and of Z^{eff} in the case of a p-doped sample of Bi_2Te_3 at $T = 300$ K: theoretical results arising from the theoretical-model equations (20).

whereas τ_p and τ_e get the same values as in Section 3.1. Moreover, since we are not aware of experimental data, in this case we still used two different values for the parameter accounting for the phonon–wall reflections (i.e., $C_p=0.1$ and $C_p=0.5$), and two different values for the parameter accounting for the electron–wall reflections (i.e., $C_e=0.1$ and $C_e=0.5$).

As it can be seen from Fig. 2, increasing values of ω lead to increasing values in both the thermal conductivity λ_p^{eff} and λ_e^{eff}, whereas the effective electrical conductivity σ_e^{eff} shows a slight decreasing behavior. We explicitly note that the opposite behaviors of λ_e^{eff} and σ_e^{eff} one finds in Fig. 2 are not against the Wiedemann–Franz law since at nanoscale, as we observed in Section 1, the characteristic-length variable allows additional control on the different material functions. The combination of these behaviors leads to an effective figure-of-merit which is substantially decreasing for increasing frequency, whatever the values of C_p and C_e are. However, the smaller the parameters accounting for the reflection of phonons and electrons at the walls, the less marked the decreasing in Z. Therefore, the theoretical model in Eqs. (6) suggests that the performances of a thermoelectric device tend to get worse in frequency-dependent situations even when the radius of the transversal section is smaller both than the phonon mfp, and than the electron one.

4. Conclusions

Thermoelectrics is a meaningful energy-conversion technology, which could generate electrical power from a temperature difference and also could produce active cooling by inputting direct electrical current. Indeed, the low energy-converting efficiency by thermoelectric system has been the bottleneck, which limited the applications to niche markets where the reliability and simplicity are more important than the performance. The revitalization of the thermoelectric industry has been due to nanotechnologies, the use of which requires a deeper scientific understanding of the physics at nanoscale. From the theoretical point of view, it is well-known, for example, that resistive, capacitive and/or inductive properties of nanomaterials show interesting time-dependent features when subject to time-dependent perturbations, but how they may influence the performances of thermoelectric devices are still an open question.

In the present paper, starting from a thermodynamic model of nonlocal transport equations for the phonon and the electron contributions to the heat flux, and for the electron contribution to the electric current, including thermoelectric effects, by means of the figure-of-merit we have analyzed how time-dependent perturbations may influence the performances of a thermoelectric device.

Since Eqs. (6) represent the basic tool of our theory, it seems advisable to spend more words about them.

Eq. (6a) is very well-known in nonequilibrium thermodynamics as the Guyer–Krumhansl (G–K) equation [25], and follows from the solution of the linearized BTE for phonons [34,7,35]. It reduces to the classical Fourier law whenever the terms $\tau_p D_t \mathbf{q}^{(p)}$ and $\ell_p^2(\nabla^2\mathbf{q}^{(p)}+2\nabla\nabla\cdot\mathbf{q}^{(p)})$ are neglected therein. Along with the observations at the very beginning of Section 2, in the present paper we assumed that the electron contribution to the local heat flux is ruled by Eq. (6b), with additional terms accounting for the Peltier effect. Whenever the terms $\tau_e D_t \mathbf{q}^{(e)}$ and $\ell_e^2(\nabla^2\mathbf{q}^{(e)}+2\nabla\nabla\cdot\mathbf{q}^{(e)})$ can be ignored in Eq. (6b), one recovers the classical equation describing the Peltier effect [36,6], namely, $\mathbf{q}^{(e)}=-(\lambda_e+\epsilon\Pi\sigma_e)\nabla T+\Pi\sigma_e\mathbf{E}$. Finally, since the electric current is produced by the electric charges moving through the crystal lattice, we also assumed that their evolution is governed by a G–K equation type, that is, Eq. (6c). That equation reduces to $\mathbf{i}=\sigma_e(\mathbf{E}-\epsilon\nabla T)$ whenever the relaxational term $\tau_i D_t\mathbf{i}$ and the second-order nonlocal contribution $\ell_e^2(\nabla^2\mathbf{i}+2\nabla\nabla\cdot\mathbf{i})$ are negligible in it.

The results contained in Ref. [37] about the compatibility of Eqs. (6) with second law of thermodynamics allow to claim that those equations do not violate any admissible physical principle.

In order to account for the interactions between heat and electric carriers and the lateral walls, in our theoretical model we complemented Eqs. (6) with suitable boundary conditions describing the wall contributions to the different diffusive fluxes. The establishment of boundary conditions in the presence of wall slip has been a subject of increasing interest in fluid mechanics, rheology and heat transport processes. In microfluidics, for example, along the lateral surfaces of a cylindrical duct it is generally supposed a slip-flow condition (i.e., the fluid velocity does not vanish along it), whereas the behavior of the fluid in the center of the duct is governed by the usual Navier–Stokes equations. In a first-order approximation, the velocity $\mathbf{v}_{\mathrm{w}}$ of the fluid on the wall of the microchannel is generally estimated as

$$\mathbf{v}_{\mathrm{w}}=cl'\frac{\partial\mathbf{v}_{\mathrm{b}}}{\partial\zeta} \tag{28}$$

wherein $\mathbf{v}_{\mathrm{b}}$ represents the velocity of the fluid in the bulk, l' is the mfp of the fluid particles, c is a positive constant related to the properties of the walls, and ζ means the outward normal direction to the boundary [38–40]. Along with the idea that the heat/electric carriers form a gas-like collection, replacing the fluid velocity with the corresponding dissipative flux $\mathbf{J}$ of the heat/electric carriers, in the case of heat transport at nanoscale from Eq. (28) one may infer that $\mathbf{J}$ on the walls is given by

$$\mathbf{J}_{\mathrm{w}}=C\ell\frac{\partial\mathbf{J}_{\mathrm{b}}}{\partial\xi} \tag{29}$$

It is easy to recognize that Eqs. (16) and (25) reduce to Eq. (29) in steady-state situations, or whenever the relaxational effects due to the interactions between the heat/electric carriers and the walls are vanishing. A rigorous theoretical study about the compatibility of Eqs. (16) and (25) may be performed as in Ref. [30] by imposing that the entropy production is non-negative not only in the bulk, but also in the bounding surface.

In the case of a cylindrical nanodevice, we have analyzed two different situations regarding the relation between the radius of the transversal section and the mfps of the different heat carriers. In both situations our theoretical model (6) predicts that Z is reduced for increasing frequency of perturbations. Indeed, our analysis suggests that nonlocal effects may be used to bring the reduction in Z down in a frequency-dependent situation. In fact, if in the synthesis and processing of a nanomaterial one is able to address the different particles at the walls in such a way that only a scant number of them suffer reflections (that is, if C_p and/or C_e get small values), than the reduction in the performance of a thermoelectric device should be attenuated in frequency-dependent situations. From this perspective, the phenomenon of backscattering [41] (i.e., the backward reflections of hitting particles at the walls), which is a huge problem for heat conduction, may be used as an aiding tool.

Acknowledgements

The author acknowledges the financial support from the Italian Gruppo Nazionale per la Fisica Matematica – GNFM.

References

[1] K.E. Goodson, M.I. Flik, Electron and phonon thermal conduction in epitaxial high-T_c superconducting films, J. Heat Trans. - T. ASME 115 (1993) 17–25.

[2] N. Stojanovic, D.H.S. Maithripala, J.M. Berg, M. Holtz, Thermal conductivity in metallic nanostructures at high temperature: electrons, phonons, and the Wiedemann–Franz law, Phys. Rev. B 82 (2010) 075418 (9 pages).
[3] A. Sellitto, V.A. Cimmelli, D. Jou, Thermoelectric effects and size dependency of the figure-of-merit in cylindrical nanowires, Int. J. Heat Mass Transf. 57 (2013) 109–116.
[4] A.I. Boukai, Y. Bunimovich, J. Tahir-Kheli, J.-K. Yu, W.A. Goddard III, J.R. Heath, Silicon nanowires as efficient thermoelectric materials, Nature 451 (2008) 168–171.
[5] G. Joshi, H. Lee, Y. Lan, X. Wang, G. Zhu, D. Wang, R.W. Gould, D.C. Cuff, M. Y. Tang, M.S. Dresselhaus, G. Chen, Z. Ren, Enhanced thermoelectric figure-of-merit in nanostructured p-type silicon germanium bulk alloys, Nano Lett. 8 (2008) 4670–4674.
[6] G. Lebon, D. Jou, J. Casas-Vázquez, Understanding Nonequilibrium Thermodynamics, Springer, Berlin, 2008.
[7] D. Jou, J. Casas-Vázquez, G. Lebon, Extended Irreversible Thermodynamics, fourth revised ed., Springer, Berlin, 2010.
[8] S. Volz (Ed.), Thermal Nanosystems and Nanomaterials (Topics in Applied Physics), Springer, Berlin, 2010.
[9] X. Wang, Z. Wang (Eds.), Nanoscale Thermoelectrics, Springer, Berlin, 2014.
[10] M.S. Dresselhaus, G. Chen, M.Y. Tang, R.G. Yang, H. Lee, D.Z. Wang, Z.F. Ren, J.-P. Fleurial, P. Gogna, New directions for low-dimensional thermoelectric materials, Adv. Mater. 19 (2007) 1043–1053.
[11] D. Nakamura, M. Murata, H. Yamamoto, Y. Hasegawa, T. Komine, Thermoelectric properties for single crystal bismuth nanowires using a mean free path limitation model, J. Appl. Phys. 110 (2011) 053702 (6 pages).
[12] D.Y. Tzou, Macro to Micro-Scale Heat Transfer. The Lagging Behaviour, Taylor and Francis, New York, 1997.
[13] Z.M. Zhang, Nano/Microscale Heat Transfer, McGraw-Hill, New York, 2007.
[14] F.X. Alvarez, D. Jou, Memory and nonlocal effects in heat transports, Appl. Phys. Lett. 90 (2007) 083109 (3 pages).
[15] Y.V. Pershin, M. Di Ventra, Memory effects in complex materials and nanoscale systems, Adv. Phys. 60 (2011) 145–227.
[16] P. Martin, Z. Aksamija, E. Pop, U. Ravaioli, Impact of phonon-surface roughness scattering on thermal conductivity of thin Si nanowires, Phys. Rev. Lett. 102 (2009) 125503 (4 pages).
[17] A. Sellitto, F.X. Alvarez, D. Jou, Phonon–wall interactions and frequency-dependent thermal conductivity in nanowires, J. Appl. Phys. 109 (2011) 064317 (8 pages).
[18] A.I. Hochbaum, R. Chen, R.D. Delgado, W. Liang, E.C. Garnett, M. Najarian, A. Majumdar, P. Yang, Enhanced thermoelectric performance of rough silicon nanowires, Nature 451 (2008) 163–167.
[19] B. Qui, L. Sun, X. Ruan, Lattice thermal conductivity reduction in Bi_2Te_3 quantum wires with smooth and rough surfaces: a molecular dynamics study, Phys. Rev. B 83 (2011) 035312 (7 pages).
[20] G. Chen, Nanoscale Energy Transport and Conversion - A Parallel Treatment of Electrons, Molecules, Phonons, and Photons, Oxford University Press, Oxford, 2005.
[21] D. Jou, V.A. Cimmelli, A. Sellitto, Nonlocal heat transport with phonons and electrons: application to metallic nanowires, Int. J. Heat Mass Transf. 55 (2012) 2338–2344.
[22] J. Zou, A. Baladin, Phonon heat conduction in a semiconductor nanowire, J. Appl. Phys. 89 (2001) 2933–2938.
[23] N.W. Ashcroft, N.D. Mermin, Solid State Physics, Saunder College, New York, 1976.
[24] Z. Lin, L.V. Zhigilei, Temperature dependences of the electron–phonon coupling, electron heat capacity and thermal conductivity in Ni under femtosecond laser irradiation, Appl. Surf. Sci. 253 (2007) 6295–6300.
[25] R.A. Guyer, J.A. Krumhansl, Thermal conductivity, second sound and phonon hydrodynamic phenomena in nonmetallic crystals, Phys. Rev. 148 (1966) 778–788.
[26] P.E. Hopkins, P.M. Norris, L.M. Phinney, S.A. Policastro, R.G. Kelly, Thermal conductivity in nanoporous gold films during electron–phonon nonequilibrium, J. Nanomater. 2008 (2008) 418050 (7 pages).
[27] G. Grimwall, The Elecron–Phonon Intercation in Metals, North-Holland Pub. Co., Amsterdam, 1981.
[28] C.B. Satterthwaite, R.W. Ure, Electrical and thermal properties of Bi_2Te_3, Phys. Rev. 108 (1957) 1164–1170.
[29] A. Sellitto, F.X. Alvarez, D. Jou, Temperature dependence of boundary conditions in phonon hydrodynamics of smooth and rough nanowires, J. Appl. Phys. 107 (2010) 114312 (7 pages).
[30] G. Lebon, D. Jou, P.C. Dauby, Beyond the Fourier heat conduction law and the thermal non-slip condition, Phys. Lett. A 376 (2012) 2842–2846.
[31] D.K. Ferry, S.M. Goodnick, Transport in Nanostructures, second ed., Cambridge University Press, Cambridge, England, 2009.
[32] D. Jou, A. Sellitto, F.X. Alvarez, Heat waves and phonon–wall collisions in nanowires, Proc. R. Soc. A 467 (2011) 2520–2533.
[33] L. Wu, A slip model for rarefied gas flows at arbitrary Knudsen number, Appl. Phys. Lett. 93 (2008) 253103 (3 pages).
[34] V.A. Cimmelli, Different thermodynamic theories and different heat conduction laws, J. Non-Equilib. Thermodyn. 34 (2009) 299–333.
[35] D.Y. Tzou, Nonlocal behavior in phonon transport, Int. J. Heat Mass Transf. 54 (2011) 475–481.
[36] S.R. De Groot, P. Mazur, Nonequilibrium Thermodynamics, North-Holland Publishing Company, Amsterdam, 1962.
[37] D. Jou, A. Sellitto, V.A. Cimmelli, Multi-temperature mixture of phonons and electrons and nonlocal thermoelectric transport in thin layers, Int. J. Heat Mass Transf. 71 (2014) 459–468.
[38] T.I. Gombosi, Gaskinetic Theory, Cambridge University Press, Cambridge, 1994.
[39] H. Struchtrup, Macroscopic Transport Equations for Rarefied Gas Flows: approximation Methods in Kinetic Theory—Interaction of Mechanics and Mathematics, Springer, New York, 2005.
[40] C. Cercignani, Slow Rarefied Flows—Theory and Application to Micro-Electro-Mechanical Systems, Birkhäuser Verlag, Basel, 2006.
[41] A.L. Moore, S.K. Saha, R.S. Prasher, L. Shi, Phonon backscattering and thermal conductivity suppression in sawtooth nanowires, Appl. Phys. Lett. 93 (2008) 083112.